ESCUELA DE CONSTRUCCIÓN CIVIL
FACULTAD DE INGENIERÍA

Revista de la Construcción
Journal of Construction

Research Article

Effect of silica fume on the microstructural and mechanical properties of concrete made with 100% recycled aggregates

Farhan Nadim[1], Rakibul Hasan[1], Md. Habibur Rahman Sobuz[2*], Jawad Ashraf[2], Noor Md. Sadiqul Hasan[3], Shuvo Dip Datta[2], Md. Hamidul Islam[4], Md. Ashraful Islam[1], Md. Robiul Awall[1], SM Arifur Rahman[5], Md. Kawsarul Islam Kabbo[2], Yaqoob Yousif Oleiwi Saif[6]

[1] Department of Building Engineering and Construction Management, Rajshahi University of Engineering and Technology, Rajshahi (Bangladesh), email: rakibulkuet14@becm.ruet.ac.bd; robi95@ce.ruet.ac.bd
[2] Department of Building Engineering and Construction Management, Khulna University of Engineering and Technology, Khulna (Bangladesh), email: habib@becm.kuet.ac.bd; jawadashraf2000@gmail.com; sd.datta@becm.kuet.ac.bd; kabbo@becm.kuet.ac.bd
[3] Department of Civil Engineering, College of Engineering and Technology, International University of Business Agriculture and Technology, Dhaka (Bangladesh), nmshasan85@gmail.com
[4] Department of Civil and Infrastructure Engineering, RMIT University, Melbourne (Australia), email: hamidcekuet@gmail.com
[5] Department Civil Engineering Discipline, School of Civil and Mechanical Engineering, Curtin University, Perth (Australia), email: rahman.Smarifur@curtin.edu.au
[6] Department of Materials and Environmental Engineering, Sfax university, Sfax (Tunisia), email: yqoobsaif997@gmail.com
* Correspondence: habib@becm.kuet.ac.bd (Md. Habibur Rahman Sobuz)

Received: 04.03.2024; **Accepted:** 04.07.2024; **Published:** 31.08.2024

Citation: Nadim, F., Hasan, R., Rahman, M., Ashraf, J., Sadiqul, N., Dip, S., Hamidul, M., Ashraful, M., Robiul, M., Arifur, S., Kawsarul, M. and Oleiwi, Y. (2024). Effect of silica fume on the microstructural and mechanical properties of concrete made with 100% recycled aggregates. Revista de la Construcción. Journal of Construction, 23(2), 413-435. https://doi.org/10.7764/RDLC.23.2.413

Abstract: Recycled concrete aggregate can be utilized in structural concrete in order to reduce the use of natural resources and the harmful impacts of waste concrete on the environment. This present research aimed to assess the effectiveness of using recycled aggregate concrete with the partial replacement of cement by silica fume (SF) to analyze the microstructural and mechanical properties of recycled aggregate concrete (RAC). In this study, recycled stone was used as coarse aggregate. The main variables of the study included the dosage of silica fume that was employed as a partial replacement of ordinary Portland cement (OPC) with four different percentages: 4%, 8%, 12%, and 16% by weight. Five different mixes were prepared, with four mixes created by varying amounts of silica fume, which were designated as RSACSF4, RSACSF8, RSACSF12, and RSACSF16. The other mix was created as a reference mix without silica fume and designated RSACSF0. Slump test was conducted to investigate the workability of concrete mixes. From the test result, a decreasing trend was found after adding more percentage of SF. Compressive and splitting tensile tests were conducted to analyze the mechanical properties of RSAC at 7 and 28 days. The results showed that the addition of SF improved the performance of RSAC at early and later curing ages, and a 12% addition of SF showed the best result. Scanning electron microscopy and X-ray diffraction analysis were performed to explore SF's microstructural performance and effect on RSAC. The results showed that silica fume showed a positive pozzolanic impact, and when combined with calcium hydroxide, it underwent a secondary hydration reaction that boosted the generation of calcium silicate hydrate and improved the parameters of the interface transition zone. X-ray diffraction analysis showed that silica fume and silica fume have similar pattern intensities. Finally, 12% SF is recommended as a partial replacement for cement in RSAC.

Keywords: Recycled concrete aggregate, mechanical performance, microstructural performance, silica fume, X-ray diffraction.

1. Introduction

Urbanization growth in developing nations has resulted in large-scale production of construction and demolition waste (CDW) in recent decades, which has had a detrimental effect on the environment. It should be mentioned that by substituting recycled aggregate for natural aggregate, the ever-increasing demand for construction can be satisfied without diminishing natural resources (Kurad et al., 2017). Additionally, adopting RA rather than NA reduces CO_2 emissions and raw materials used during the production of structural members (H. He, J. Shi, et al., 2024). The reduction of carbon footprints in the environment will add extra points and thus enhance the concrete industry. On the other hand, over the past few years, the volume of waste generated during the construction and demolition phases has significantly increased (Rana et al., 2022; Sobuz et al., 2023). CDW must be stored, managed, and turned into an expensive recycled aggregate (RA) before it can be used in construction (Datta et al., 2022; Sobuz, Datta, & Rahman, 2022). New forms of aggregates must be found immediately because NAs are non-renewable resources.

CDW has been seen in this context as a potential source of aggregate. These leftovers from CDW can be processed into recycled coarse aggregates (RCAs) after a specific process (Iqbal et al., 2020). Many nations have established policies and procedures for recycling waste materials for use in construction, and many nations have also started turning construction wastes into RA. Conventional CDW disposal methods, such as piling it up or dumping it in landfills, result in substantial environmental degradation and increased storage space requirements (Lavado et al., 2020). CDW includes natural stone, leftover concrete, bricks, and other materials that actually belong to the renewable materials category. Today, recycling construction waste into recycled aggregates for use as concrete, or recycled aggregate concrete (RAC), is regarded as a sustainable solution that lowers environmental pollution and raw material consumption (Sobuz, Datta, Akid, et al., 2022). Old mortar covering the RA's surface significantly impacts the RAC's interface transition zone (ITZ). On the surface of the RA, ITZ exists between the new and old mortar, but it also exists between the NA and new mortar (Lee et al., 2013). As a result, finding effective and easy ways to enhance the mechanical features of ITZs having old cement mortar at curing ages is crucial to developing the strength of RAC and utilizing RAC widely in building engineering. Because adherent mortar in RAs is usually substantially weaker than new cement pastes and natural aggregate and the weakest zone in RAC is the porous ITZ (Huang, Li, Yuan, et al., 2022; Saravanakumar et al., 2016; Wei et al., 2023). Concrete has been a staple of the construction industry for more than a century because of its adaptability, simplicity in shaping, and low cost (Huang, Li, Zhang, et al., 2022; Huang, Yuan, Zhang, & Zhu, 2021; Wei et al., 2023). It is among the most often used building materials.

Cement, fine aggregates (such as sand), and coarse aggregates are mixed with water to create concrete, which eventually becomes hard (Aditto et al., 2023). The most popular type of cement for making concrete is called Portland cement. Many types of cement are employed to create concrete with a variety of characteristics and uses. Concrete has been a staple of the construction industry for more than a century because of its adaptability, simplicity in shaping, and low cost (Pang et al., 2024; Sobuz, Al, et al., 2024; Sobuz, Joy, et al., 2024). Some varieties of cement include Portland pozzolana cement (PPC), cement that hardens quickly, cement that is resistant to sulfates, and others. To achieve a certain strength, materials are combined in a specified ratio. The water-cement ratio has a significant impact on a variety of qualities, including strength, workability, and durability. A sufficient water-cement ratio is necessary for the creation of usable concrete. When water and other ingredients are combined, cement reacts with the water, and the hydration process begins. This reaction aids in forming a solid matrix that holds the constituent parts together to generate a long-lasting substance that resembles stone.

Only a few factors that affect concrete strength include the caliber of the raw materials, the coarse/fine aggregate ratio, the water-to-cement ratio, the age of the concrete, the temperature, the level of compaction, the curing process, and the relative humidity. One of the potential options involves turning CDW into concrete aggregate. CDW has a negative environmental impact; thus, using recycled aggregate in concrete will assist in lessening that impact. An analysis of statistical data revealed that China created 15 billion tons of construction debris in 2015 (Hasan et al., 2022). The need for construction aggregate is also anticipated to increase to up to 47 billion tons yearly. One of the most important things the construction industry does to help preserve the environment and promote long-term sustainability is to find new uses for the waste it generates. The longer

these materials last, the less garbage is dumped, and the fewer trees are cut down (Cui et al., 2024). However, the extraction of natural resources like sand and gravel for construction projects can alter the course of rivers and their beds, raising environmental problems (Huang, Yuan, Zhang, & Li, 2021; Zhang et al., 2024). Although the worldwide construction industry promotes the use of recycled aggregates in the production of concrete, this is mostly done to address the issue of the depletion of natural aggregates.

However, SF has a greater impact on the compressive behavior of RAC than fly ash and powdered granulated blast furnace slag (Jin et al., 2024). Metal refining generates a byproduct called smelter's flux (SF) (Corinaldesi et al., 2009). Because of its pozzolanic impact and micro-filler properties, SF can change the mechanical properties of concrete by strengthening the link between the cement paste and aggregates in the ITZ (H. He, E. Shuang, et al., 2024; Song et al., 2024). Interestingly, Sobuz et al. 2022 also concluded that the application of SF might result in a bigger and more significant improvement in the mechanical qualities of RAC than NCA (Sobuz, Datta, Akid, et al., 2022). This may be associated with the increased interface transition zones and the higher w/c ratio that results from the high-water absorption rate of the RCA's ITZ. An analysis of recycled concrete reveals three distinct interface transition zones: 1) the layer separating the old mortar from the new mortar, 2) the layer separating the aggregates from the old mortar, and (optionally) 3) the layer separating the recycled aggregate from the new mortar. Given that the transition layer lies at the concrete's weakest structural point. It is possible for resistance to change, either decreasing or increasing, depending on the RCAs and the needs of the reference concrete in which the recycled aggregate was employed (Khan et al., 2023; Wu et al., 2024).

Researchers have examined, for instance, how steel fiber and silica fume impact the mechanical properties and impact behavior of concrete built with two distinct types of recycled coarse aggregates. (Nazarimofrad et al., 2017) found that all recycled aggregate concrete' split tensile and compressive strengths were significantly impacted by the use of silica fume and steel fibers at the same time, most likely as a result of the steel fibers' improved adhesion to the silica fume-containing mortar and the mortar's improved ITZ with the RCA. Comparing the RAC to conventional samples, Benemaran et al. discovered that adding glass fibers and silica fume increases the tensile strength of the samples' compressive and splitting strengths (Benemaran et al., 2024). There are several impacts of silica fume on the properties of RAC studied in order to increase the effectiveness of using recycled concrete as an aggregate. Mirza and Saif (2010) conducted an experiment about the replacement rates for natural aggregate with recycled aggregate, which were 0, 50, and 100% by weight. Silica fume was used to replace cement to the extent of 5, 10, and 15% also by weight (Rahman Sobuz, Alam, et al., 2023). The findings demonstrated that grade 40/50 MPa recycled aggregate concrete can be produced successfully. As compressive and splitting tensile strength values were noted at all ages, the best combination for RAC is composed of 100% recycled aggregate content and 5% SF as a partial replacement. On the other hand, numerous researchers summarized a systematic approach to determine how recycled coarse aggregate affected RAC's mechanical properties and workability (L. He et al., 2024; Younis et al., 2021; Zhao et al., 2024).

Additionally, the effects of silica fume (SF) in place of cement on RAC performance were examined. Four percentages of silica fume (5%, 10%, 15% and 20%) were used. Silica fume can be utilized at contents of (10–20%) of cement mass to obtain mechanical performance for the RAC comparable to the concrete using NCA. (H. Dilbas et al. 2014) conducted an experimental investigation to assess the mechanical and physical characteristics of recycled aggregate concrete (RAC) with and without silica fume (SF). In this investigation, recycled aggregate (RA) with and without SF is employed in concrete compositions made from destroyed building rubble. The ideal ratio for RA in concrete mixtures is 30 percent for improved results. It has been discovered that adding 5% SF to RAC makes it easier to improve its weaker qualities, including compressive strength. An experimental study was conducted by (Rahman Sobuz, Meraz, et al. (2023) to find out how silica fume (SF) and particles of rubber could work together to improve the compressive strength of treated steel-fiber recycled aggregate concrete was also rubberized (Fang et al., 2024; Wei et al., 2024; Xie, Huang, et al., 2018).

The primary test parameters were SF and rubber contents. In order to evaluate RSRAC's carbon emissions, we conducted a series of axial compression tests to analyze its compressive strength, energy dissipation capacity, elasticity modulus, and failure cause. The compressive strength of RSRAC is improved by incorporating SF due to the fortification of weak interfacial connections between the RCA, steel fiber, rubber particles, and cement paste. This strength is affected by the amount of SF present. It is discovered that RSRAC, having 100% recycled coarse aggregate with 5% rubber and 10% SF, produces the best

results when compressive characteristics and carbon emissions are taken into account synthetically. The research was conducted to study the mechanical behavior of rubberized steel-fiber recycled aggregate concrete (RSRAC) modified with silica fume in order to design RSRAC safely and cost-effectively. From the perspective of the synthetic study of mechanical improvement and manufacturing costs, the RSRAC with 10% silica fume and 5% rubber for structural elements appear to be more sustainable than normal concrete. According to Amnon Katz's investigation, the microscopic makeup of recycled material is made by smashing old concrete (Katz, 2004). It was found that the recycled aggregate is covered with loose particles, which can prevent a solid binding between the recycled aggregate and the new cement matrix. The recycled aggregate's mechanical properties were subpar due to the previous cement paste, which remained on the natural aggregate and was porous and fractured. The recycled aggregate compressive strength rose by 15% and by 23–33% at ages 7 and 28 days after being impregnated, respectively, with 10% by weight silica fume treatment. Singh et al. (2019) demonstrated in their study that M30 grade of self-compacting concrete (SCC) having recycled aggregate at various percentages of 0%, 50%, 75%, and 100% and different percentages of silica fume had good compressive strength, good abrasion resistance, and good chloride penetration resistance (0%, 5%, 10%, and 15%).

Results were contrasted with SCC, which is typical. It was found that replacing recycled aggregates with 50% and silica fume with 10%, respectively, led to the greatest gain in compressive strength and durability. In another study, authors described the impacts of adding silica fume (SF) to the concrete mix design to raise the caliber of recycled aggregates used in concrete (Çakır & Sofyanlı, 2015). SF was substituted for Portland cement at 0%, 5%, and 10%. According to tests on compressive strength, tensile splitting strength, water absorption, and ultrasonic pulse velocity, using 10% SF as a cement replacement for recycled aggregate concretes increased concrete's hardened and physical properties. Sasanipour et al. provided an experimental study in which silica fume was employed as a component of cementitious materials in order to enhance the qualities of self-compacting concrete (SCC), which was manufactured with fine and coarse recycled aggregates (Sasanipour & Aslani, 2020). Concrete with used, recycled, or demolished coarse material is called recycled aggregate concrete (RAC). Although using RCA to make RAC is better for the environment and sustainability, its performance is not as good as natural aggregate concrete (NAC) (Evangelista & De Brito, 2007). RAC contains higher internal microcracks and porosity than NAC (Pradhan et al., 2020). Due to the low application rate of RAC, one of the key factors affecting its mechanical properties is the replacement rate of RA (Feng et al., 2022).

The performance of RAC is reportedly worse than that of NAC. Concrete, in both its fresh and hardened states, is affected by RCA (Younis & Pilakoutas, 2013). Concrete's mechanical qualities and ability to be worked are both reduced by RCA. Compressive, splitting tensile, and flexural strength of concrete may all be reduced by up to 40%, 25%, and 20%, respectively, when compared to NAC (Younis et al., 2014). According to various research, recycled concrete aggregates are distinct from natural aggregates because they are made of two materials. In contrast, natural aggregate is one of two and is coupled with cement mortar. The sorptivity test results of Hameed et al.'s investigation into the water absorption characteristics of concrete made with RAC indicated that the compression casting technique positively affected the water absorption characteristics of low-grade 100% RAC. Results also indicated that, in comparison to concrete mixes with natural aggregates, RAC mixes had poorer water absorption qualities (Hameed et al., 2022). The findings of the studies conducted by Silva et al. (2021) indicate that RCA causes a loss in the SCC's fluidity, flow rate, passing ability, and filling capacity and that high percentages (75% and 100%) of RCA exhibit the largest reduction in workability.

It has been discovered from an experiment that at recycled aggregate utilization levels of 25–50%, little or no negative effects were noticed on the strength, workability, or fracture characteristics. It was shown that the compressive and flexural strengths, as well as the elastic modulus of RAC, dropped in comparison to those of standard concrete as the replacement rate of recycled aggregate rose (Mills-Beale et al., 2010). The recycled aggregate's high porosity, high water absorption, and low strength are the main causes of this. The only noticeable consequence was a slight decrease in Young's modulus (Grdic et al., 2010; Rao et al., 2011). The main determinant was the dose of Nano silica, which included 0%, 1.5 %, and 3 % of cement content with unit weights of 400 and 450 Kg/m^3. The outcomes were contrasted using straightforward concretes. The concretes' mechanical and microstructural characteristics (as determined by a SEM test) were examined. After conducting the investigation, it was determined that using 100% recycled materials instead of coarse natural aggregates reduced compressive strength by 15% to 20%. Compressive strengths for Nano silica concrete are higher than those for normal concrete by a factor of 3%. The lower workability of concrete resulted from the increase in the amount of nano silica and recycled particles. (Tang

Yunchao et al., 2021) demonstrated that the addition of SF only strengthens RAC later. In contrast, the significant pozzolanic activity of NS can strengthen RAC earlier, in which compression and splitting tensile tests were conducted to examine the mechanical properties of RAC having SF-NS induced at different ages after curing.

The mechanical properties of concrete remain largely unaffected by replacement levels of up to 30% of NCA by RCA, as demonstrated by published research (Jahandari et al., 2021). Furthermore, the surface qualities and characteristics of coarse aggregates have a significant impact on the microstructure of the interfacial transition zone (ITZ) (Qudoos et al., 2018). The literature review conducted in the author's prior study (Qudoos et al., 2018) leads one to conclude that ITZ is crucial for regulating the mechanical and durability-related characteristics of concrete. However, more research is needed to address durability issues and encourage broader application of this sustainable concrete using RCA to develop viable solutions for waste management and environmentally friendly building (Sinduja Joseph et al., 2023).

Prior studies primarily looked at substituting natural aggregate content for recycled aggregate and not 100% RAC; very little research was done on the splitting patterns and microstructure analysis of 100% RAC with SF. In this work, recycled coarse aggregate made from demolished concrete waste is employed in the concrete compositions along with siliceous sand. The mechanical characteristics, such as compressive strength and tensile splitting strength, as well as the microstructural characteristics, such as the ITZ between cement paste and concrete and porosity, have been developed for this purpose using thirty concrete mixtures divided into five groups. The objective of this research is to examine the observed splitting patterns from splitting tensile and compressive strength tests, as well as the effects of the mechanical and fresh properties of 100% RCA concrete with 0%, 4%, 8%, 12%, and 16% replacement percentages of SF. Additionally, this study examines the microstructure characteristics of RAC at various percentages of silica fume replacement at 7 and 28 days. Our research's novelty lies in this analysis, which has never been done before with 100% RCA concrete.

2. Materials and methods

Locally available ordinary Portland cement (OPC) was used in this research work. It conforms to the Bangladesh standard BDS EN 197-1:2003 CEM-I 42.5 N and 52.5 N, European Standard EN 197 type CEM I, and American standard ASTM C 150 Type-I mark. It contains Portland clinker: 95-100% and gypsum: 0-5%. The specific surface area of cement was 388 m^2/kg. Table 1 represents the chemical composition of cement. The coarse aggregate used for this study was collected from available local suppliers. Recycled coarse aggregate obtained from demolished concrete slabs, which were later crushed, with a maximum particle size of 20 mm, was used in this study. In all test procedures, an ASTM standard sieve size of 10 mm was retained, and 4.75 mm passing stone chips were used to prepare the mixes. In this study, Sylhet sand was used and collected from the local market. The physical properties of aggregates, such as fineness modulus, specific gravity, moisture content, void ratio, and loose and compacted bulk density, were determined according to the standards set out by ASTM C136/C136M-19, ASTM C127-15, ASTM C566, ASTM C128-15, ASTM C29/ C29M_17a respectively. The values of the property tests for fire aggregate and coarse recycled stone are shown in Table 1.

Table 1. Physical properties of aggregates.

Parameter	Fine aggregate	Coarse aggregate
Fineness modulus	2.61	7.31
Specific gravity	2.63	2.78
Moisture content (%)	1.83	2.01
Loose density (kg/m^3)	1465	1457
Bulk density (kg/m^3)	1555	1572
Void ratio (%)	40.75	43.33

Silica fume was collected from the ‘NEOTECH construction chemical company Ltd, Dhaka’. An ultrafine powder has been collected as a byproduct of the manufacture of silicon and ferrosilicon alloys. The chemical compositions of the OPC and silica fume are shown in Table 2.

Table 2. Chemical properties of silica fume.

Constituents	Weight (%) OPC	Weight (%) silica fume
SiO_2	19.01	89.94
Al_2O_3	4.58	0.51
Fe_2O_3	3.20	0.65
CaO	66.89	0.75
MgO	1.26	1.52
Na_2O	1.205	0.21
MnO	0.19	-
K_2O	2.76	0.47
SO_2	0.45	0.09
Loss of ignition (LOI)	1.235	5.26

2.1. Experimental program

2.1.1. Mix proportion

The basic mix composition of the concrete comprised a 1:1.9:2.50 ratio by volume of Ordinary Portland Cement, fine aggregate, and coarse aggregate. The ratio of water to binder was set as 0.46 in this study. Silica fume was also used as a mineral admixture. Practically, the mix proportions can change depending on the characteristics of the individual elements and the desired attributes of the concrete in service. The different concentrations of silica fume used as a cement substitute led to different concrete mix designations at the rate of 0%, 4%, 8%, and 16%. Five concrete mixes have been done with respect to the silica fume percentage variation shown in Table 3. The control mix was done with 0% silica fume and identified as RSACSF-0, and the other mixes were identified as RSACSF-4, RSACSF-8, RSACSF-12, and RSACSF-16. All authorized concrete mixes were mixed in accordance with ASTM C685 guidelines. The concrete mixes were prepared manually. At first, cement and sand and the required percentage of silica fume are mixed until they are of the same color. Then, the mixture was poured down into stones and mixed with a spade. After that, a small pit was dug into the mixture, and water was poured accordingly. Then, the mixture was mixed from outside to inside until it reached the desired consistency. When mixing manually, 10% extra cement was used.

Table 3. Mix proportion of concrete.

Mix. type	Cement (Kg/m^3)	Water	W/C	Fine aggregate (silica sand) (Kg/m^3)	Coarse aggregate (recycled stone) (Kg/m^3)	Silica fume (%)
RSACSF-0 (Reference)	386	185	0.46	762	1006	0
RSACSF-4	371	185	0.46	762	1006	4
RSACSF-8	355	185	0.46	762	1006	8
RSACSF-12	340	185	0.46	762	1006	12
RSACSF-16	325	185	0.46	762	1006	16

2.1.2. Sample preparation and curing

The concrete prepared was poured in steel molds, which were oiled with proper lubricant material. Three equal layers of newly mixed concrete were poured into the molds, and each layer was tamped 25 times with a 16 mm tamping rod. Excess concrete was formed on the top of the mold and smoothened without imposing pressure on it. A total number of 60 concrete mixes were prepared. They consisted of 30-cube specimens and 30-cylinder specimens prepared for overall tests. For the splitting tensile strength test, the cylinder was prepared sized 152 mm X 304 mm, and for the compressive strength test, the cube was prepared sized 152 mm X 152 mm X 152 mm. The concrete mix IDs were stated as RSACSF-0, RSACSF-4, RSACSF-8, RSACSF-12, and RSACSF-16 with silica fume of 0%, 4%, 8%, 12% and 16% of cement weight accordingly. Afterward, the specimens were put at room temperature for hardening. After 24-36 hours, they were demolded and placed in a curing tank with lab-supplied tap water. Subsequently, they were cured for 7 and 28 days, and tests were performed accordingly on those days. Figure 1 shows the preparation of the specimens.

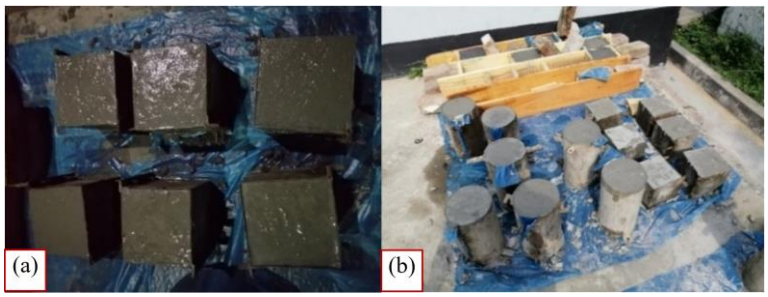

Figure 1. Preparation of the specimens (a) cube (b) cylinder.

2.1.3. Mechanical and microstructural properties testing

ASTM C143 was followed for conducting the Slump test. This test was carried out to ascertain whether freshly mixed concrete was workable in compliance with the standard. To further understand the impact of substituting silica fume for cement on the workability of the concrete, slump tests were performed on all of the replacement options. It is found that the slump value for M30 to M40 concrete can be taken as a minimum of 50 and a maximum of 100.

According to the ASTM C140 standard applied in this investigation, the cubic specimen underwent a compressive strength test. Equation (1) was used to determine the test results after the calibration of the testing device. The testing device could support 3000 kN. The plates underwent a thorough cleaning. 20 cubes of 152 x 152 mm were tested for compressive strength at 7 and 28 days after casting. The compressive testing machine was used to apply the compression load in a single direction. The load was applied continuously and uninterruptedly with a constant force of 0.25 MPa/s. On the basis of the failure load readings, compressive strength was determined.
The formula for calculating the compressive strength of a cube is shown in equation (1) below.

$$C_s = {}^{P}/_{A} \qquad (1)$$

where, P = load (N), A = area (mm^2)

According to the ASTM C496 standard, the cylinder specimen used in this investigation underwent split tensile testing. The same equipment from the previous test was utilized to evaluate compressive strength. Up until failure, the sample was subjected to a continuous rate of diametric compressive loading. Figure 2 depicts the test configuration. The sample experiences tensile failure when tensile stress is applied to the plate carrying the imposed load. After 7 and 28 days of curing, 20 cylinders of 304 x 152 mm were removed from the water and tested for tensile strength.

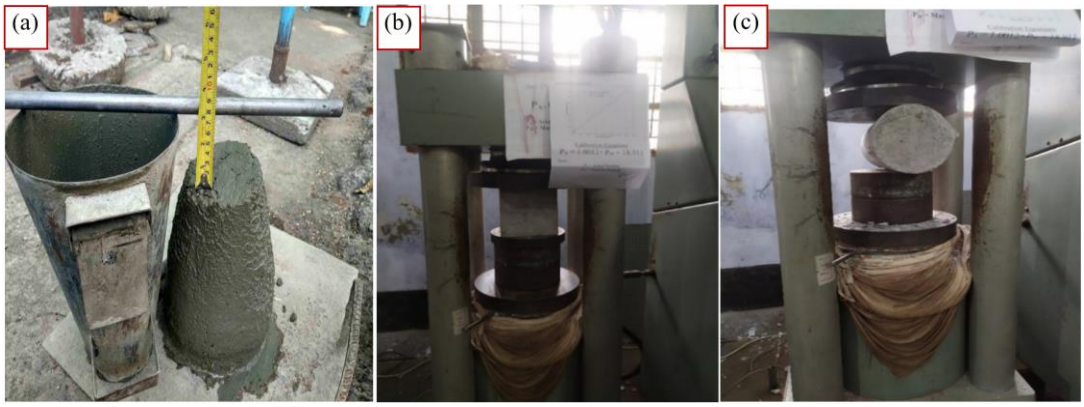

Figure 2. Experimental setup (a) slump test (b) compressive strength test (c) splitting tensile strength test.

The microscopic structure of the recycled aggregate concrete sample with varied amounts of silica fume was examined using scanning electron microscopy (SEM). The specimen was broken down into small pieces sized around 2 cm for conducting the test. The test was conducted in JCM-6000Plus versatile benchtop SEM. XRD analyses of those powders were performed using diffractometer with Cu radiation over the range 10–80° and 2θ, step size of 0.02° and scan speed of 2 degree/min. Silica fume and cement of about 5gm were given for this test to conduct.

3. Experimental results and analysis

3.1. Rheological properties

3.1.1. Slump test result

The changes in slump values with the addition of silica fume in RSAC are demonstrated in Figure 3. From this graphical representation, it is seen that the slump values decrease with the increase in silica fume percentages. 26.16%, 20%, 10.77%, and 7.69% linear declination of slump values were found for RSACSF4, RSACSF8, RSACSF12, and RSACSF16 mixes over control mix, respectively. Silica fume sticks the ingredients of concrete together because of its cementitious properties, and it would be the first cause of the reduction of slump value. When recycled aggregate is processed, the surface roughness is also increased, which tends to lessen the flow characteristics and decrease the slump value. More specifically, resistance mobility and grain locking in concrete could happen due to the rough texture and uneven shape of RSACSF. The decreasing trends of slump value with the inclusion of silica fume in concrete have also been observed by findings from some researchers (Duval & Kadri, 1998; Hosseini et al., 2011; Younis et al., 2021)

It is found by Younis, Alzeebaree et al. (2021) that the addition of up to 20% silica fume content in concrete decreases the slump value from 110 mm to 55 mm. Hosseini, Rahman Sobuz, Alam, et al. (2023) stated in their study that the addition of Nano silica in concrete decreases the slump value from 120 mm to 30 mm (Hosseini et al., 2011). Duval et al. showed in their study that the addition up to 10% silica fume to partial cement replacement has no effect on the workability of concrete (Duval & Kadri, 1998). Rahman Sobuz, Meraz, et al. (2023) also found that fresh concrete has less workability to a certain point after the addition of micro-silica. However, the slump value of all the concrete mixes stayed within the desired slump range of 20 mm to 100 mm, which is suggested by (ASTM, 2015).

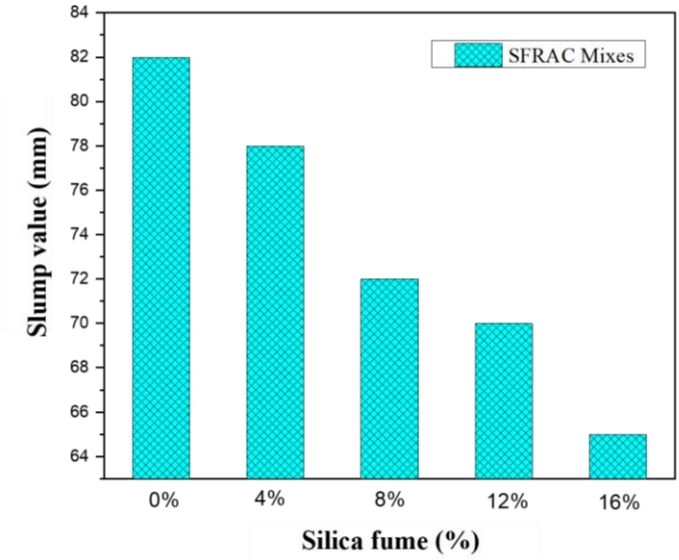

Figure 3. Slump value for different % of silica fume.

3.2 Hardened properties

3.2.1. Effects of silica fume on compressive strength

The findings of the compressive strength test are summarized in Table 4, which includes the standard deviation, mean strength, coefficient of variation (COV), standard error, and lower and upper bounds at a 95 percent confidence interval. Notably, three samples of each percentage of silica fume were examined in a lab, and the mean value was determined using the compressive strength test findings at 7 and 28 days. According to the statistical analysis, the concrete specimens' compressive strengths at all curing ages ranged from 19.63 MPa to 31.39 MPa. When tested after 7 days, the control mix's compressive strength ranged from 19.63 to 19.89 MPa, whereas after 28 days, it tested between 31.20 to 31.39 MPa. The concrete specimen's standard deviation ranges from 0.112 to 0.087, with a COV of 0.57 to.28 percent, and the standard error varies from 0.064 to 0.50. With a 95% confidence interval of 19.63 MPa to 19.89 MPa, RSACSF-0's compressive strength is the lowest at 19.76 MPa at 7 days, and RSACSF-16 compressive strength is the highest at 21.58 MPa at 7 days, with a 95% confidence interval of 21.37 MPa to 21.78 MPa. In contrast, the compressive strength of 28-days for RSACSF-0 has the lowest value of 30.08 MPa with a 95% confidence interval of 29.91 MPa to 30.25 MPa and the highest value of 32.03 MPa at 28-day specimen with 95% confidence interval of 31.78 MPa to 32.28 MPa. The results of this study show that adding silica fume with concrete gradually increases its strength. However, a 12% addition of silica fume shows better results than a further addition of silica fume at 28 days. Bajpai et al. (2020) reported that the inclusion of silica fume in the range of 5 to 25% in concrete increases its compressive strength from 6% to 30%. Also, the highest co-efficient of variance identified from Table 4 is 0.855% for the RSACSF-12 mix, and the lowest co-efficient of variance is found as 0.136% for the 8 percent incorporation of SF. The usages of silica fume at different levels have significantly affected the standard deviation of all RSACSF mixes. However, this may not always be the case due to material properties, environmental conditions, and the various parameters used in various studies.

Table 4. Regression summary of the compressive strength test result.

Mixes	Days	Mean strength (MPa)	Standard deviation	COV (%)	Standard error	95% confidence interval	
						Lower range	Upper range
RSACSF-0	7	19.76	0.112	0.566	0.064	19.63	19.89
	28	30.08	0.152	0.505	0.087	29.91	30.25
RSACSF-4	7	20.34	0.078	0.383	0.045	20.25	20.43
	28	30.20	0.121	0.469	0.069	30.06	30.33
RSACSF-8	7	20.52	0.028	0.136	0.016	20.48	20.60
	28	31.12	0.162	0.513	0.093	30.94	31.30
RSACSF-12	7	21.36	0.176	0.823	0.102	21.16	21.56
	28	32.03	0.220	0.855	0.127	31.78	32.28
RSACSF-16	7	21.58	0.182	0.843	0.105	21.37	21.78
	28	31.29	0.087	0.278	0.050	31.20	31.39

After curing those specimens for 7 and 28 days, the compressive test was conducted. For the control and RSACSF mix, Figure 4 shows the variation in mean compressive strength from the data of 3 specimens of each mix. From Table 4, it is observed that the compressive strength of RSACSF specimens at 7 days is between 59.90 and 62.13% of the strength of concrete specimens at 28 days. The illustration of Figure 4 shows that the concrete made from recycled stone and silica fume performed admirably by giving the needed strength, and the highest value was found 32.05 MPa for RSACSF-12 mix, which consists of 12% silica fume. From Figure 4, it is seen that adding 16% silica fume decreases the strength compared with the previous one. The study clearly showed that SFRAC had higher compressive strength than control concrete specimens after 7 and 28 days of curing.

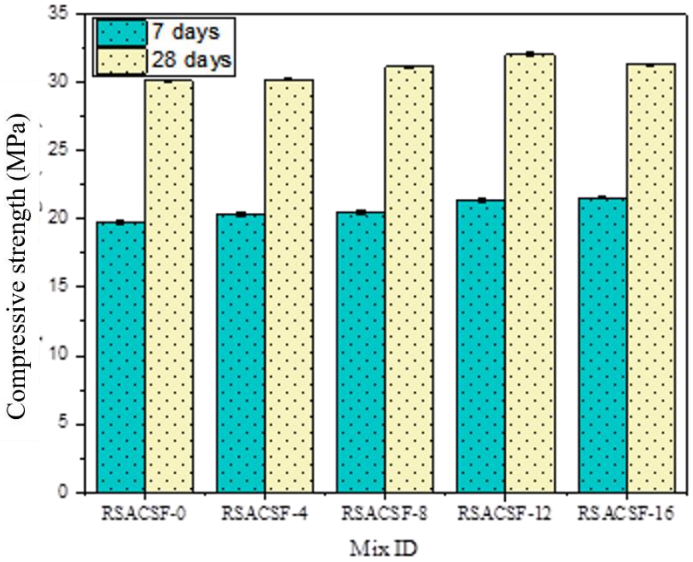

Figure 4. Compressive strength test results of the concrete mixes at 7 and 28 days.

Figure 5 demonstrates that at 28 days, the progressive percentage change in compressive strength of RSACSF relative to the control mix is greater for silica fume concentrations of more than 12%. The highest ideal silica fume level in this investigation is, therefore, 12%. Yunchao et al. (2021) showed in his study that the strength rose with age for concrete under 28 days and peaked at 2 percent for children older than that. The compressive strength of RAC was reduced with a low NS concentration of 1% when the RA replacement was 50%. NS improved the compressive strength of RAC at early curing ages for a 100% RA substitution. Compressive strength of SFRC at various ages often shows a tendency of first declining, then increasing, and lastly decreasing with an increase in the amount of SF. This indicates that SFRC characteristics are impacted by abnormally low or high SF levels. By adding silica fume, the compressive strength is improved by up to 11.23%. After taking into account the 28-day compressive strength test, the 12% incorporation rate is the one for the SFRAC mixtures that were determined to be optimal.

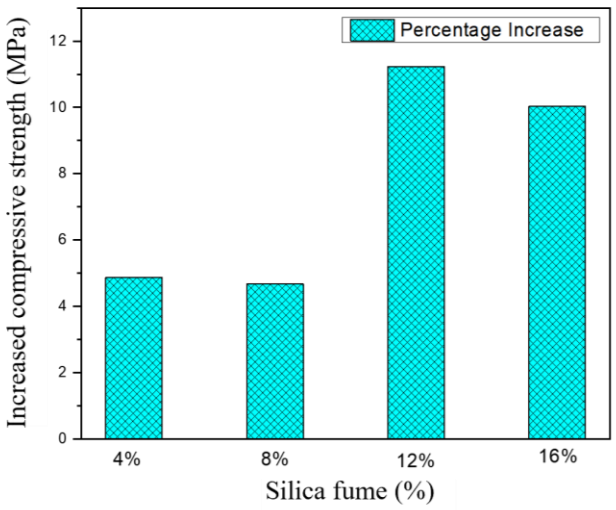

Figure 5. Increase of compressive strength of the concrete mixes.

Figure 6 depicts the failure patterns caused by compression testing of cylindrical control and RSACSF specimens with varying concentrations of silica fume over a 28-day testing period. Within seconds of the peal stress being reached in the cubic specimens of RSACSF-4 and RSACSF-8, an angled fracture wedge surface is created. As a result, concrete began to

spall, which is depicted in Figure 6(b) as the so-called cone and shear failure mode (c). It is evident that the cubic specimens lose more energy depending on the severity of cracking in this wedge formation. The sample fracture pattern demonstrated the silica fume's confining impact in conjunction with the crushed recycled stone used as aggregate, which tends to hold the materials together and has the opposite effect of lateral stress. Again, cone and shear failure were detected by specimens (a) and (c), having the mix ID of RSACSF-16 and RSACSF-8, as indicated in Figure 6. The smaller aggregates spall out from the mortar bonding due to cement matrix particles, and this behavior is similar to that of previous experimental studies (Das et al., 2020). In Figure 6 (d), microcracks were seen in RSACSF-12 after the ultimate load had been implemented.

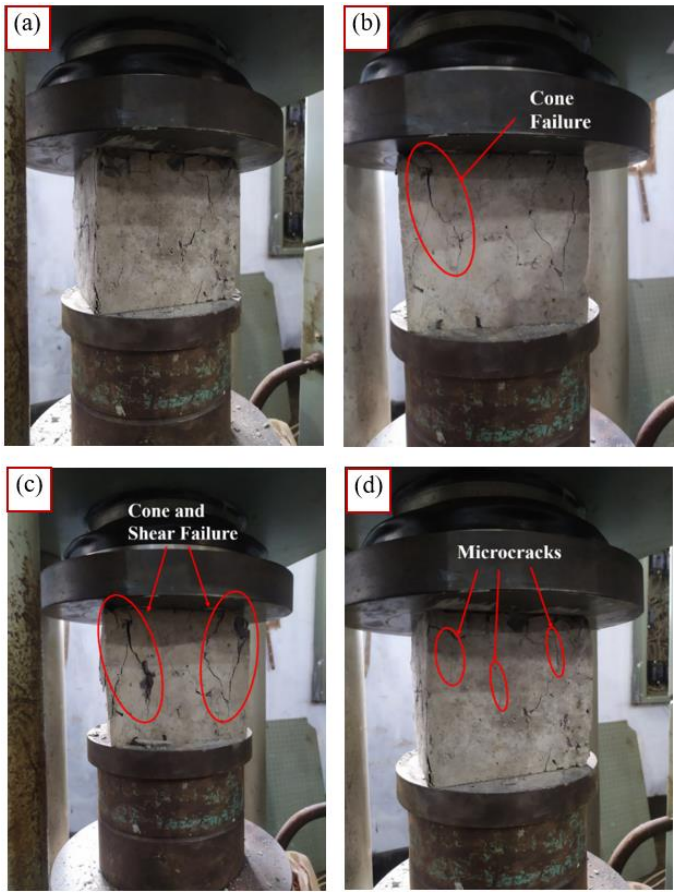

Figure 6. Observed compressive strength failure patterns of the specimen at 28 days of (a) RSACSF-16 (b) RSACSF-4 (c) RSACSF-8 and (d) RSACSF-12.

3.2.2 Effects of silica fume on splitting tensile strength

The results of the splitting tensile strength test, which were summarized in Table 5, were examined using a variety of statistical methods to determine the mean strength, standard deviation, coefficient of variation (COV), standard error, and the lower and higher range at a 95% confidence interval. It should be mentioned that three samples of each silica fume percentage were evaluated in a lab setting, and the mean value was determined using the results of the tests for splitting tensile strength at 7 and 28 days. According to the statistical analysis, the concrete specimens' splitting tensile strength ranged from 1.55 MPa to 3.14 MPa at all curing ages. At 7 days, the splitting tensile strength of the control mix ranged from 1.55 to 1.60 MPa, while at 28 days, the strength of the control mix was ranged from 3.09 to 3.14 MPa. The standard deviation of concrete specimens ranges from 0.019 to 0.025, with the corresponding COV of 1.20% to .80%, and the standard error ranges from 0.010 to 0.83. The splitting tensile strength has the lowest value of 1.58 MPa at 7-days specimen with 95% confidence interval of 1.55 MPa to 1.60 MPa and has the highest value of 2.01 MPa at 7-days specimen with 95% confidence interval of 1.84 MPa to 2.17

MPa. In contrast, the splitting tensile strength of the 28-day specimen has the lowest value of 2.64 MPa with a 95% confidence interval of 2.57 MPa to 2.61 MPa and the highest value of 3.26 MPa at the 28-day specimen with a 95% confidence interval of 3.19 MPa to 3.33 MPa. Also, the highest co-efficient of variance identified from Table 4.2 is 4.78% for the RSACSF-12 mixture, and the lowest co-efficient of variance is found as 0.80% for the RSACSF-16 mix. According to the ACI code, the tensile strength of concrete should be around 10% of the compressive strength, and in this investigation, it was found to be around 7-8%; however, for low-strength concrete, it can vary up to 11-12% (Brettmann et al., 1986). Due to the characteristics of the materials, the surrounding environment, and the many criteria utilized in different research, this might not always be the case.

Table 5. Regression summary of the split tensile strength test result.

Mixes	Days	Mean strength (MPa)	Standard deviation	COV (%)	Standard error	95% confidence interval	
						Lower range	Upper range
RSACSF-0	7	1.58	0.019	1.20	0.010	1.55	1.60
	28	2.64	0.059	2.23	0.034	2.57	2.71
RSACSF-4	7	1.60	0.044	2.75	0.025	1.56	1.65
	28	2.78	0.028	1.00	0.093	2.74	2.61
RSACSF-8	7	1.69	0.049	2.89	0.028	1.64	1.64
	28	3.01	0.042	1.39	0.014	2.93	3.06
RSACSF-12	7	1.82	0.087	4.78	0.050	1.72	1.72
	28	3.26	0.061	1.87	0.020	3.19	3.33
RSACSF-16	7	2.01	0.142	3.06	0.082	1.84	2.17
	28	3.12	0.025	0.80	0.083	3.09	3.14

The concrete cubes were tested after 7 days and 28 days of curing. Figure 7 reflects the variation of mean splitting tensile strength for control and SFRAC mix from the data of 3 specimens of each mix. It illustrates the results of the splitting tensile strength test of the concrete mix with and without silica fume. It is found from the study that after 7 and 28 days of curing, RSACSF-16 showed maximum strength of 2.04 MPa at 7 days and RSACSF-12 showed highest splitting tensile strength of 3.36 MPa at 28 days. From Figure 7, it is also observed that adding more silica fumes tends to decrease splitting tensile strength.

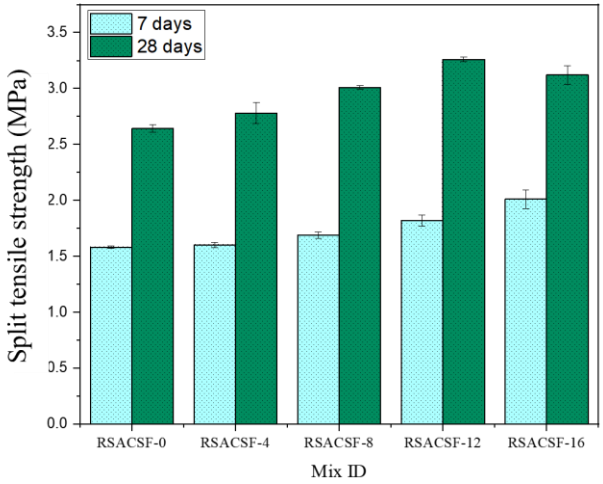

Figure 7. Splitting tensile strength of the concrete mixes at 7 and 28 days.

Figure 8 shows that for silica fume concentrations larger than 12 percent, the progressive percentage change in splitting tensile strength of RSACSF relative to the control mix is greater at 28 days. Therefore, 12% is this inquiry's recommended silica fume level. The lower value of the split tensile strength is caused by the decreased cohesive force between the RSCA surfaces and cement matrix, which enhances the lower binding tendency in the concrete mix. This conclusion is consistent

with the findings of past tests (Khademi et al., 2016). According to Thomas et al., the loss in the concrete's splitting tensile strength is between 2 percent and 8 percent when RCA is approximately 25% of the total, which is fairly similar to the study (Das et al., 2020). However, González-Fonteboa and Martínez-Abella (2008) observed that the reduction in splitting strength that occurs when natural aggregate is replaced with recycled aggregate can be minimized by adding nanoparticles of silica fume to the concrete mix. This increase is, therefore, also applicable to the recommended 12 percent inclusion of silica fume(González-Fonteboa & Martínez-Abella, 2008).

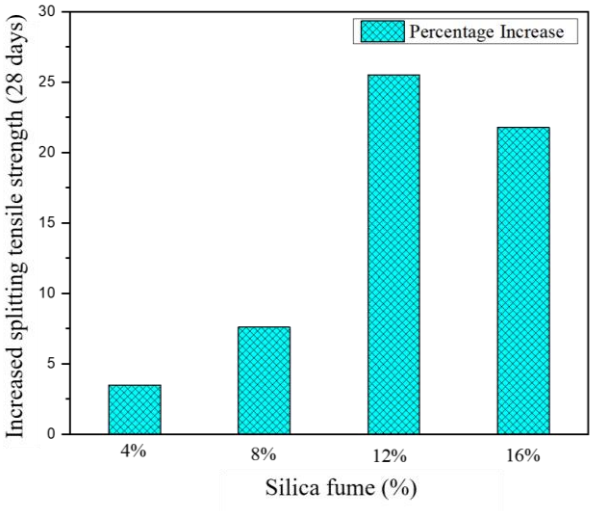

Figure 8. Increase of splitting tensile Strength of the concrete mixes.

Figure 9 shows the cylindrical specimens splitting tensile testing failure patterns with varying silica fume percentages caused by replacement of cement in RSAC at 28 days of testing. Failure patterns were taken into consideration for further research on concrete strength and to comprehend how to use this mix according to protocol. Additionally, the microstructural morphology can be improved from the crack pattern to improve future properties of this kind of cement replacement in concrete. When the crack appeared in the center of the cylinder diameter under uniaxial stress, as illustrated in Figures 9(a) and (b), it can be seen that the Control and RSACSF mix specimen failed in a less brittle manner. When the major crack first emerged, the crack pattern was torn apart. If the failure type is further examined, it becomes clear from Figure 4.6 that the major crack for RSACSF-16 was initially started. However, when strength levels rise, the toughness increases and flattens off. According to the aggregate type, more energy is needed to fracture an aggregate of a particular size. This is due to the fact that the fracturing process may be significantly influenced by the strength, stiffness, shape, and surface texture of the aggregate type. It should be noticed that the primary crack in the concrete specimen's crack pattern was visible when the specimen split apart. When the primary crack appeared, it divided the crack pattern apart. When looking more closely at the failure type, it is apparent from Figure 9 (d) that the major crack for RSACSF-16 was started first. As strength levels rise, however, the toughness increases flatten off. An aggregate's type has a direct relationship with the energy needed to fracture it at a given size. This is due to the possibility that the strength, stiffness, shape, and surface texture of the aggregate type may all have a substantial impact on the fracturing process. It should be noticed that the specimen's major crack was where the concrete specimen's crack pattern could be seen.

According to Feng et al. (2021), the specimens with 0% RA replacement exhibited a large number of large inclined cracks and numerous microscopic microcracks, which are comparable with the failure patterns of ordinary concrete. It demonstrated that when RAC was subjected to compressive loads, SF and NS could effectively prevent the development of cracks. In a different investigation, Xie, Fang, et al. (2018) revealed unmistakably that concrete cylinders containing 10% SF generated substantial longitudinal macrocracks, whereas concrete cylinders devoid of SF displayed a huge number of smaller longitudinal cracks. These outcomes could be explained by how the rise in silica fume dramatically altered the microstructure of the calcium silicate hydrate (C-S-H) gel, creating a denser interface between the cement matrix and the PPF or steel fiber, all of

which increase the brittleness of the concrete while improving bonding performance and preventing crack propagation (Fang et al., 2024; Jabin et al., 2024). The creation of stronger ITZs as a result of the SF's pozzolanic and filler activities may be the primary cause of the phenomenon (Dilbas et al., 2014).

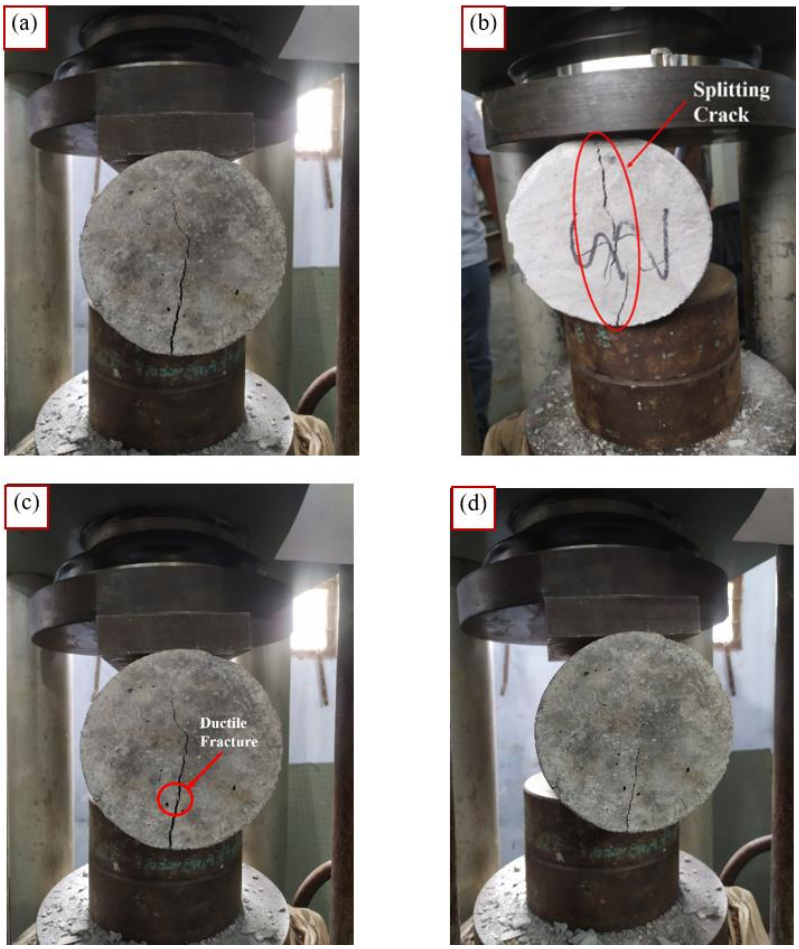

Figure 9. Observed Splitting tensile strength failure patterns of the specimen at 28 days of (a) RSACSF-4 (b) RSACSF-8 (c) RSACSF-12 (d) RSACSF-16.

3.2.3 Relationship between compressive and splitting tensile strength

As shown in Figure 10, the test results for the split-tensile and compressive strength exhibit a good coefficient of correlation and regression for the current study. It has been noted that the tensile strength of concrete is between 8% and 10% of its compressive strength. Additionally, the tensile strength of RCA mixtures significantly improves as compressive strength increases, and these improvements remain almost constant throughout the investigation. However, ACI code "Building code requirements for structural concrete (ACI 318-08) and commentary" (2008) exhibits the furthest estimation from the confidence band and prediction band of the experimental outcomes. It is evident that the equation of CEB-FIP (Comite Euro-International Du, 1993) and AS 3600 (Standard, 2001) are near enough forecasts to the current 95% prediction band of the specimens. The ACI 363R-92 code (Committee, 1984) covers substantial portions of the prediction zone, and in comparison to other codes of standards, it demonstrates a good estimate. Due to the inclusion of the ultrafine silica fume in the concrete mixes, the high splitting tensile strength generates the upward forecast line from the other standards. Moreover, the interlocking action of the aggregates improves the splitting tensile strength characteristics of the concrete mixes.

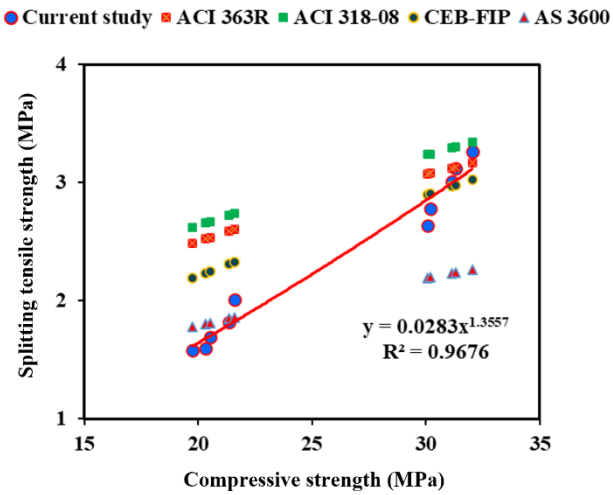

Figure 10. Relationship between compressive and splitting tensile strength.

3.2.4 Effects of silica fume on microstructural properties

Figure 11 presents the graphical presentation of the findings from the scanning electron microscopy (SEM) Test. Figure 11 (a) shows the microstructure of RSACSF-0 at 7 days in which micropores are being seen. Those voids were formed because the old cement mortar of recycled stone aggregates absorbed cement particles on their surface. As a result, these varieties of concrete have a somewhat higher ITZ porosity than traditional concrete. Figure 10 (b) depicts the microstructure of RSACSF-0 specimen without silica fume at 28 days. It can be noticed that there are a lot of crumbs on the surface, as shown in Figure 11 (b). The crumbs range in size from a few microns to several hundred microns and are only loosely connected to the main aggregate. These debris pieces most likely resulted from the old cement paste and concrete being pulverized (Mueller & Winkler, 1998). The lower left of Figure 11(b) and the upper left of Figure 11 both show the old cement matrix that encircles the new aggregate surface from the old concrete (a). Microcracks and damage to the cement matrix generated by tension from the crushing process are depicted in Figure 11(a). RSACSF-0's degraded and more porous old cement matrix is inferior to samples (b). The new aggregate surface from the old concrete is surrounded by an old cement matrix, which is visible. Two elements appear to have a detrimental effect on the quality of the recycled aggregates in addition to the w/c ratio of the previous cement matrix. These include coating aggregates with loose particles and breaking up the original cement matrix, which reduces the mechanical strength of the recycled aggregate. The bond between the recycled aggregate and the new cement matrix is weakened. While silica nanoparticles have reduced even very small holes in the transition zone of recycled concrete, making it denser and more uniform, it is clear from comparing figures 11 (c) and (d) and 11 (e) and (f) that they have not completely eliminated these holes. This is especially true because nanoparticles perform differently than other materials. The inner microstructure of the specimen was denser than that of the specimen with 12 percent silica fume, as shown in Figure 4.8. It follows from these results that the chemical reaction between silica fume and $Ca(OH)_2$ produced C-S-H gel, which can fill vacuum spaces (Bui et al., 2018). RSACSF-12 mixes at 28 days show more compactness at the micro level than RSACSF-12 mixes at 7 days. Physical filling and chemical filling are two different types of the filling effect. The internal voids of the cement paste and the compactness of the RSAC were both significantly improved by the activation of silica fume. Furthermore, NS, acting as an activator, accelerated the cement's hydration, changed the degree of CH's orientation in the ITZ, and reacted with CH to generate a low-density C-S-H gel, which filled the pores and densely filled the interior structure (Ji, 2005). The main reason for the transition zone's higher uniformity and density is that these particles undergo a pozzolanic reaction with calcium hydroxide crystals ($Ca(OH)_2$) to create dense calcium-silicate-hydrate gelatin. In fact, it can be concluded from the SEM images in Figures 11(c), (d), (e), and (f) that the mortars containing NS powder had fewer pores overall than the mortars containing no NS powder. The most significant compressive and tensile strength were obtained with 12% and 16% replacement of SF with cement which occurred due to the dense interior structure of the concrete specimens, as seen by the SEM analysis. This further proves the benefits of using SF to improve concrete performance. This explanation is consistent with that of Blanco et al., who found that because silica fume has a smaller particle size, it acts as a filler (Blanco

et al., 2006). More C-S-H gel is produced by the SF's pozzolanic reaction and expands into the capillary spaces left behind after the cement in mortar mixes hydrates.

X-ray diffraction test was conducted on cement and silica fume samples, which is illustrated in Figure 12. Peaks resembling those of tricalcium silicate (C_3S), dicalcium silicate (C_2S), tricalcium aluminate (C_3A), and tetra calcium alumino-ferrite (C_4AF) can be seen in the XRD pattern of OPC. Additionally, it was discovered that the silica fume XRD pattern had generally amorphous features. From the chemical composition of these materials, the highest peak is obtained for SiO_2 for silica fume and CaO for cement. Since there is more periodicity in one direction than the other and some peaks have a high intensity, the diffraction peak of C-S-H is found to be almost the same for both specimens. Some peaks are tall because of a desired crystal orientation, while others are short because the crystals are put in an arbitrary order. The intensity of the plane reflected in the XRD pattern increases with increasing electron density variation.

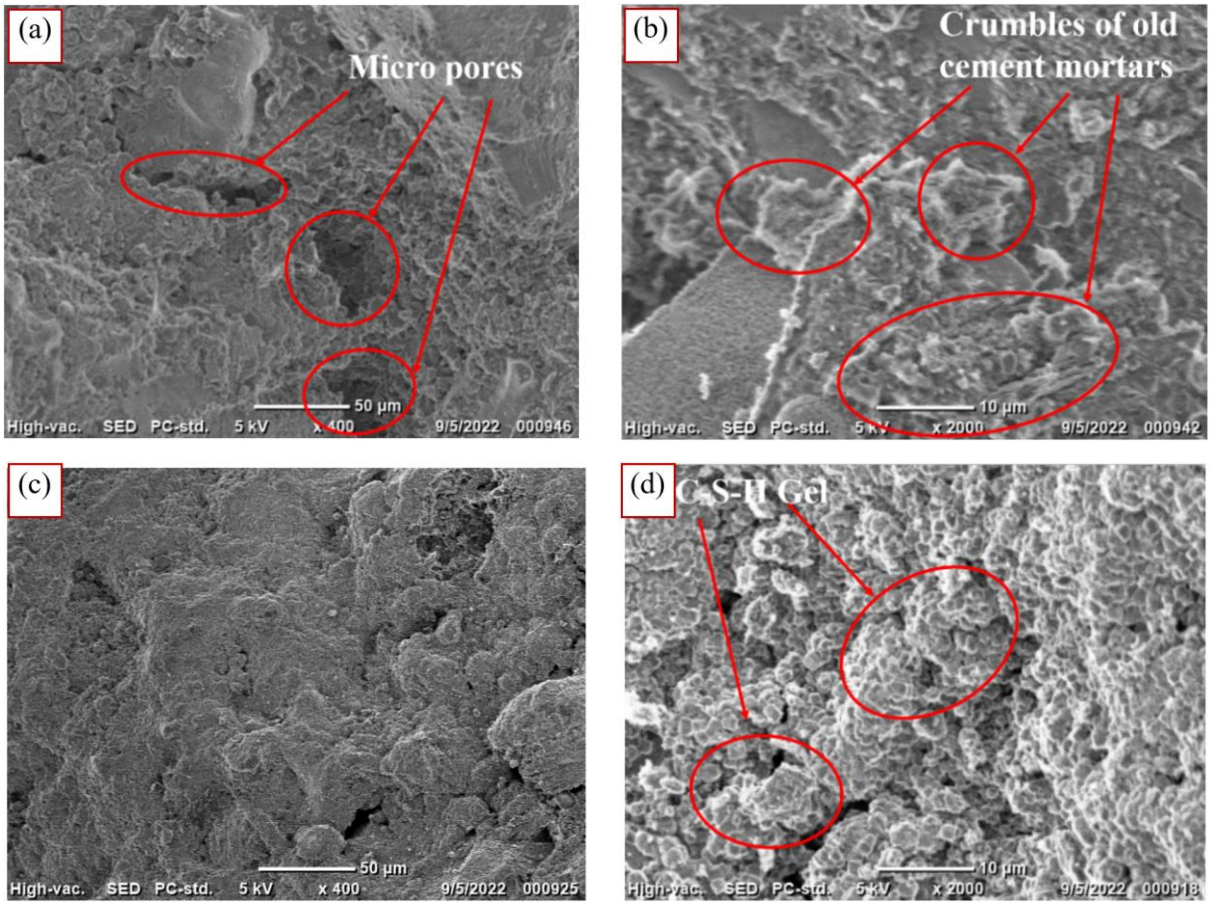

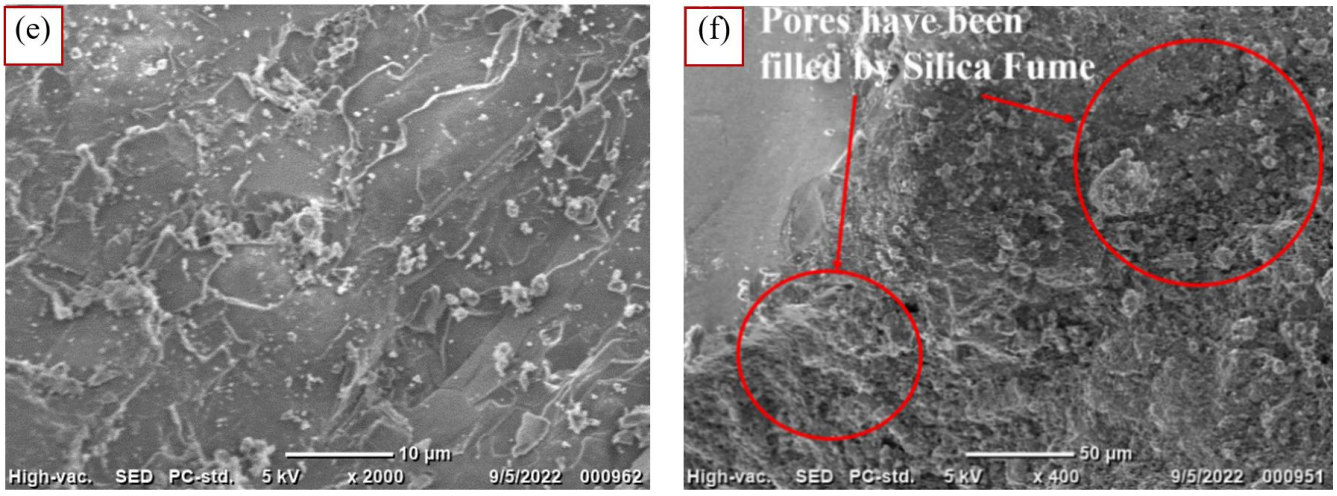

Figure 11. Microstructure of specimens from SEM analysis (a) RSACSF-0 (7 days) (b) RSACSF-0 (28 days) (c) RSACSF-12 (7 days) (d) RSACSF-12 (7 days) (e) RSACSF-12 (28 days) (f) RSACSF-12 (28 days).

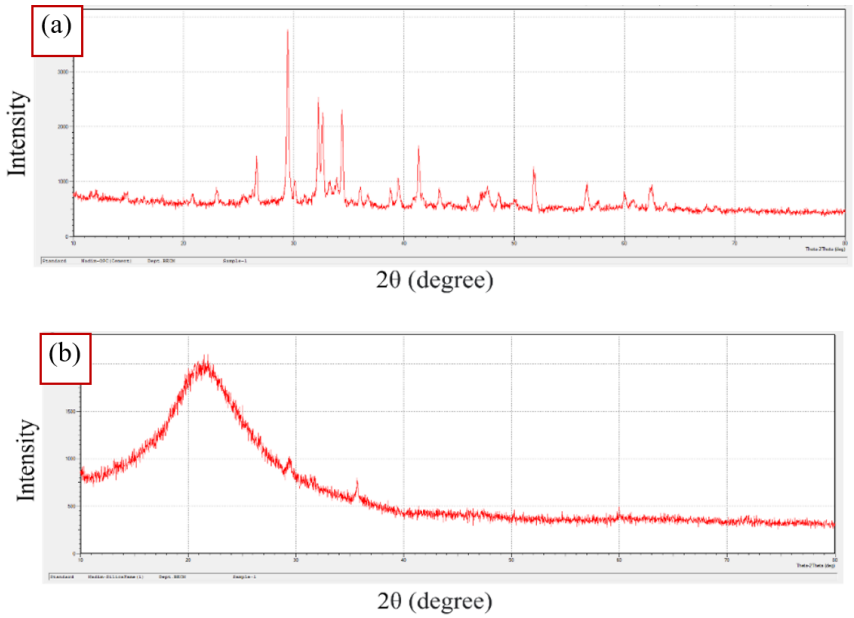

Figure 12. (a) XRD pattern of OPC (b) XRD pattern of silica fume.

4. Conclusions and Future Recommendation

In this research work, five concrete mixes with varying percentages of silica fume inclusion were tested to investigate how silica fume performed as a partial replacement for cement in recycled aggregate. Additionally, an experimental program was run to assess the mechanical and microstructural characteristics of recycled aggregate concrete when silica fume was present. The obtained mechanical and microstructural properties are concluded as follows:

1. The slump values of RSACSF mixes ranged from 65 mm to 82 mm. The higher silica fume percentage in RSAC also results in mixes with a higher density and lower workability. The surface roughness is also raised during the processing of recycled aggregate, which tends to reduce the slump value and flow characteristics. Due to its

cementitious qualities, silica fume binds the components of concrete together and is the primary factor causing the slump value to decrease.

2. The compressive strength of concretes containing RCA was enhanced by the sequential addition of SF. The compressive strength of recycled aggregate concrete has been strongly influenced by mixtures with varied concentrations of silica fume replacement. However, the recycled aggregate's rough and pointed edges help to increase interlocking, which results in a strong bond between them. However, from the test, it is found that the compressive strength increases by 11.23% compared to the control mix. RSACSF12 mixes of 12% silica fume of 28 days show maximum compressive strength of 32.05 MPa. The control specimen's low strength may be due to the presence of loose mortar around the recycled aggregate, which prevents proper bonding between cement paste and aggregate. Silica fume facilitates the C-S-H bond formation between cement and aggregate particles due to its pozzolanic properties.
3. Split tensile strength was also found increased about 25.5% compared to reference mix which is greater compared to compressive strength. SFRAC12 mixes of 12% silica fume of 28 days shows maximum split tensile strength of 3.36 MPa. Increasing the SF percentage above 12% decreases the strength. Strength declines because SF is unable to bind free calcium hydroxide with sufficient water in the matrix to produce more calcium silicate hydrate gels.
4. From SEM analysis, it is found that mixes with silica fume fill the micro pores of the structure and make the structure more compact than the mix in which silica fume was not used. Compared to the control specimen, the microstructures of the transition zones in the concrete specimens that produced silica fume were denser. Additionally, the formation of C-S-H bonds increased with curing age, contributing to an increase in compressive strength. Concrete surfaces benefited from an extended curing period because fewer pores were observed. The pores were filled with silica fume, creating a more uniform structure.
5. The denser interface strengthened bonding and stopped crack propagation as SF content rose, but it also made the concrete more ductile. Therefore, compared to the control, fewer longitudinal cracks were observed at failure patterns for SF specimens. We can, therefore, conclude that adding silica fume to recycled aggregate concrete will enhance its performance.
6. It is recommended that, in order to improve the mechanical and durability properties of building materials, the construction industry investigate the possibility of combining other pozzolanic materials, such as fly ash, marble powder, and metakaolin, into 100% RAC. To optimize its effectiveness, the ideal percentage of pozzolanic materials needs to be carefully considered. Machine learning techniques can be employed to determine the optimal percentage for achieving maximum strength in concrete. Future work focusing on CO_2 emissions and economic analysis is also recommended in order to achieve environmentally friendly and sustainable construction.

Author contributions: Conceptualization: Farhan Nadim, Rakibul Hasan, Md. Habibur Rahman Sobuz, Noor Md. Sadiqul Hasan, Md. Hamidul Islam, Md. Ashraful Islam, Md. Robiul Awall.

Methodology: Farhan Nadim, Rakibul Hasan, Md. Habibur Rahman Sobuz, Jawad Ashraf, Noor Md. Sadiqul Hasan, Md. Md. Hamidul Islam, Md. Ashraful Islam, Md. Robiul Awall.

Software: Farhan Nadim, Rakibul Hasan, Md. Habibur Rahman Sobuz, Noor Md. Sadiqul Hasan, Shuvo Dip Datta, Md. Ashraful Islam, Md. Robiul Awall.

Validation: Farhan Nadim, Rakibul Hasan, Md. Habibur Rahman Sobuz, Noor Md. Sadiqul Hasan, Md. Ashraful Islam, Md. Robiul Awall, SM Arifur Rahman.

Formal Analysis: Farhan Nadim, Rakibul Hasan, Md. Habibur Rahman Sobuz, Jawad Ashraf, Noor Md. Sadiqul Hasan, Md. Hamidul Islam, Md. Ashraful Islam, Md. Robiul Awall, Md. Kawsarul Islam Kabbo.

Investigation: Farhan Nadim, Rakibul Hasan, Md. Habibur Rahman Sobuz, Md. Ashraful Islam, Md. Robiul Awall.

Resources: Farhan Nadim, Rakibul Hasan, Md. Habibur Rahman Sobuz, Noor Md. Sadiqul Hasan.

Data Curation: Farhan Nadim, Rakibul Hasan, Md. Habibur Rahman Sobuz, Jawad Ashraf, Shuvo Dip Datta, Md. Hamidul Islam, Md. Ashraful Islam, Md. Kawsarul Islam Kabbo, Yaqoob Yousif Oleiwi Saif

Writing—original draft preparation: Farhan Nadim, Rakibul Hasan, Md. Habibur Rahman Sobuz, Jawad Ashraf.

Writing—review and editing: Farhan Nadim, Rakibul Hasan, Md. Habibur Rahman Sobuz, Noor Md. Sadiqul Hasan, Jawad Ashraf, Md. Hamidul Islam, Md. Ashraful Islam, SM Arifur Rahman, Md. Kawsarul Islam Kabbo.

Visualization: Rakibul Hasan, Md. Habibur Rahman Sobuz, Noor Md. Sadiqul Hasan, Md. Robiul Awall, Yaqoob Yousif Oleiwi Saif

Supervision: Rakibul Hasan, Md. Habibur Rahman Sobuz.

Project administration: Rakibul Hasan, Md. Habibur Rahman Sobuz

Funding acquisition: Rakibul Hasan, Md. Habibur Rahman Sobuz

Funding: This research received no external funding.

Acknowledgments: The authors would like to show gratitude to the technicians, lab-attendant and other associates for supporting during fabrication of specimens and machine operations. The authors also gratefully appreciate the personnel associated with the Department of Civil Engineering, Rajshahi University of Engineering & Technology, Rajshahi-6204, Bangladesh.

Conflicts of interest: The authors declare no conflict of interest.

References

Aditto, F. S., Sobuz, M. H. R., Saha, A., Jabin, J. A., Kabbo, M. K. I., Hasan, N. M. S., & Islam, S. (2023). Fresh, mechanical and microstructural behaviour of high-strength self-compacting concrete using supplementary cementitious materials. Case Studies in Construction Materials, 19, e02395.

ASTM, C. (2015). C143-C143M-15a Standard Test Method for Slump of Hydraulic-Cement Concrete. Book of ASTM Standards, 1–4.

Bajpai, R., Choudhary, K., Srivastava, A., Sangwan, K. S., & Singh, M. (2020). Environmental impact assessment of fly ash and silica fume based geopolymer concrete. Journal of Cleaner Production, 254, 120147.

Benemaran, R. S., Esmaeili-Falak, M., & Kordlar, M. S. (2024). Improvement of recycled aggregate concrete using glass fiber and silica fume. Multiscale and Multidisciplinary Modeling, Experiments and Design, 7(3), 1895–1914. https://doi.org/10.1007/s41939-023-00313-2

Blanco, F., Garcia, M. P., Ayala, J., Mayoral, G., & Garcia, M. A. (2006). The effect of mechanically and chemically activated fly ashes on mortar properties. Fuel, 85(14-15), 2018–2026.

Brettmann, B. B., Darwin, D., & Donahey, R. C. (1986, 1986). Bond of reinforcement to superplasticized concrete.

Bui, N. K., Satomi, T., & Takahashi, H. (2018). Effect of mineral admixtures on properties of recycled aggregate concrete at high temperature. Construction and Building Materials, 184, 361–373.

ACI Committee, 318. "Building code requirements for structural concrete (ACI 318-08) and commentary." American Concrete Institute, 2008. Çakır, Ö., & Sofyanlı, Ö. Ö. (2015). Influence of silica fume on mechanical and physical properties of recycled aggregate concrete. HBRC journal, 11(2), 157–166.

Comite Euro-International Du, B. (1993). CEB-FIP MODEL CODE 1990: DESIGN CODE. http://www.icevirtuallibrary.com/doi/book/10.1680/ceb-fipmc1990.35430

Committee, A. (1984, 1984). State-of-the-art Report on High-strength Concrete (ACI 363R-84).

Corinaldesi, V., & Moriconi, G. (2009). Influence of mineral additions on the performance of 100% recycled aggregate concrete. Construction and Building Materials, 23(8), 2869-2876. https://doi.org/https://doi.org/10.1016/j.conbuildmat.2009.02.004

Cui, D., Wang, L., Zhang, C., Xue, H., Gao, D., & Chen, F. (2024). Dynamic Splitting Performance and Energy Dissipation of Fiber-Reinforced Concrete under Impact Loading. Materials, 17(2), 421. https://www.mdpi.com/1996-1944/17/2/421

Das, S., Habibur Rahman Sobuz, M., Tam, V. W. Y., Akid, A. S. M., Sutan, N. M., & Rahman, F. M. M. (2020). Effects of incorporating hybrid fibres on rheological and mechanical properties of fibre reinforced concrete. Construction and Building Materials, 262, 120561. https://doi.org/https://doi.org/10.1016/j.conbuildmat.2020.120561

Datta, S. D., Sobuz, M. H. R., Akid, A. S. M., & Islam, S. (2022). Influence of coarse aggregate size and content on the properties of recycled aggregate concrete using non-destructive testing methods. Journal of Building Engineering, 61, 105249. https://doi.org/https://doi.org/10.1016/j.jobe.2022.105249

Dilbas, H., Şimşek, M., & Çakır, Ö. (2014). An investigation on mechanical and physical properties of recycled aggregate concrete (RAC) with and without silica fume. Construction and Building Materials, 61, 50–59.

Duval, R., & Kadri, E. H. (1998). Influence of silica fume on the workability and the compressive strength of high-performance concretes. Cement and concrete Research, 28(4), 533–547.

Evangelista, L., & De Brito, J. (2007). Mechanical behaviour of concrete made with fine recycled concrete aggregates. Cement and Concrete Composites, 29(5), 397–401.

Fang, B., Qian, Z., Song, Y., Diao, X., Shi, T., Cai, X., & Wang, L. (2024). Evaluation of early crack resistance performance of concrete mixed with ternary minerals using temperature stress testing machine (TSTM). Journal of Cleaner Production, 465, 142780. https://doi.org/https://doi.org/10.1016/j.jclepro.2024.142780

Feng, W., Liu, F., Yang, F., Jing, L., Li, L., Li, H., & Chen, L. (2021). Compressive behaviour and fragment size distribution model for failure mode prediction of rubber concrete under impact loads. Construction and Building Materials, 273, 121767.

Feng, W., Wang, Y., Sun, J., Tang, Y., Wu, D., Jiang, Z., Wang, J., & Wang, X. (2022). Prediction of thermo-mechanical properties of rubber-modified recycled aggregate concrete. Construction and Building Materials, 318, 125970.

González-Fonteboa, B., & Martínez-Abella, F. (2008). Concretes with aggregates from demolition waste and silica fume. Materials and mechanical properties. Building and Environment, 43(4), 429–437. https://doi.org/https://doi.org/10.1016/j.buildenv.2007.01.008

Grdic, Z. J., Toplicic-Curcic, G. A., Despotovic, I. M., & Ristic, N. S. (2010). Properties of self-compacting concrete prepared with coarse recycled concrete aggregate. Construction and Building Materials, 24(7), 1129–1133.

Hameed, R., Un-Nisa, Z., Riaz, M. R., & Gillani, S. A. A. (2022). Effect of compression casting technique on the water absorption properties of concrete made using 100% recycled aggregates. Revista de la construcción, 21(2), 387–407.

Hasan, N. M. S., Sobuz, M. H. R., Khan, M. M. H., Mim, N. J., Meraz, M. M., Datta, S. D., Rana, M. J., Saha, A., Akid, A. S. M., Mehedi, M. T., Houda, M., & Sutan, N. M. (2022). Integration of Rice Husk Ash as Supplementary Cementitious Material in the Production of Sustainable High-Strength Concrete. Materials, 15(22), 8171. https://www.mdpi.com/1996-1944/15/22/8171

He, H., Shi, J., Yu, S., Yang, J., Xu, K., He, C., & Li, X. (2024). Exploring green and efficient zero-dimensional carbon-based inhibitors for carbon steel: From performance to mechanism. Construction and Building Materials, 411, 134334. https://doi.org/https://doi.org/10.1016/j.conbuildmat.2023.134334

He, H., Shuang, E., Lu, D., Hu, Y., Yan, C., Shan, H., & He, C. (2024). Deciphering size-induced influence of carbon dots on mechanical performance of cement composites. Construction and Building Materials, 425, 136030. https://doi.org/https://doi.org/10.1016/j.conbuildmat.2024.136030

He, L., Chen, B., Liu, Q., Chen, H., Li, H., Chow, W. T., Tang, J., Du, Z., He, Y., & Pan, J. (2024). A quasi-exponential distribution of interfacial voids and its effect on the interlayer strength of 3D printed concrete. Additive Manufacturing, 89, 104296. https://doi.org/https://doi.org/10.1016/j.addma.2024.104296

Hosseini, P., Booshehrian, A., & Madari, A. (2011). Developing concrete recycling strategies by utilization of nano-SiO 2 particles. Waste and Biomass Valorization, 2, 347–355.

Huang, H., Li, M., Yuan, Y., & Bai, H. (2022). Theoretical analysis on the lateral drift of precast concrete frame with replaceable artificial controllable plastic hinges. Journal of Building Engineering, 62, 105386. https://doi.org/https://doi.org/10.1016/j.jobe.2022.105386

Huang, H., Li, M., Zhang, W., & Yuan, Y. (2022). Seismic behavior of a friction-type artificial plastic hinge for the precast beam–column connection. Archives of Civil and Mechanical Engineering, 22(4), 201. https://doi.org/10.1007/s43452-022-00526-1

Huang, H., Yuan, Y., Zhang, W., & Li, M. (2021). Seismic behavior of a replaceable artificial controllable plastic hinge for precast concrete beam-column joint. Engineering Structures, 245, 112848. https://doi.org/https://doi.org/10.1016/j.engstruct.2021.112848

Huang, H., Yuan, Y., Zhang, W., & Zhu, L. (2021). Property Assessment of High-Performance Concrete Containing Three Types of Fibers. International Journal of Concrete Structures and Materials, 15(1), 39. https://doi.org/10.1186/s40069-021-00476-7

Iqbal, M. F., Liu, Q.-f., Azim, I., Zhu, X., Yang, J., Javed, M. F., & Rauf, M. (2020). Prediction of mechanical properties of green concrete incorporating waste foundry sand based on gene expression programming. Journal of hazardous materials, 384, 121322. https://doi.org/https://doi.org/10.1016/j.jhazmat.2019.121322

Jabin, J. A., Khondoker, M. T. H., Sobuz, M. H. R., & Aditto, F. S. (2024). High-temperature effect on the mechanical behavior of recycled fiber-reinforced concrete containing volcanic pumice powder: An experimental assessment combined with machine learning (ML)-based prediction. Construction and Building Materials, 418, 135362. https://doi.org/https://doi.org/10.1016/j.conbuildmat.2024.135362

Jahandari, S., Mohammadi, M., Rahmani, A., Abolhasani, M., Miraki, H., Mohammadifar, L., Kazemi, M., Saberian, M., & Rashidi, M. (2021). Mechanical properties of recycled aggregate concretes containing silica fume and steel fibres. Materials, 14(22), 7065.

Ji, T. (2005). Preliminary study on the water permeability and microstructure of concrete incorporating nano-SiO2. Cement and concrete Research, 35(10), 1943–1947.

Jin, Z., Li, M., Pang, B., Yang, L., Chen, Y., & Wang, D. (2024). Internal superhydrophobic marine concrete: Interface modification based on slag microstructure regulation. Journal of Building Engineering, 86, 108769. https://doi.org/https://doi.org/10.1016/j.jobe.2024.108769

Katz, A. (2004). Treatments for the Improvement of Recycled Aggregate. Journal of Materials in Civil Engineering, 16(6), 597-603. https://doi.org/10.1061/(ASCE)0899-1561(2004)16:6(597)

Khan, M. M. H., Sobuz, M. H. R., Meraz, M. M., Tam, V. W. Y., Hasan, N. M. S., & Shaurdho, N. M. N. (2023). Effect of various powder content on the properties of sustainable self-compacting concrete. Case Studies in Construction Materials, 19, e02274. https://doi.org/https://doi.org/10.1016/j.cscm.2023.e02274

Kurad, R., Silvestre, J. D., de Brito, J., & Ahmed, H. (2017). Effect of incorporation of high volume of recycled concrete aggregates and fly ash on the strength and global warming potential of concrete. Journal of Cleaner Production, 166, 485–502. https://doi.org/https://doi.org/10.1016/j.jclepro.2017.07.236

Lavado, J., Bogas, J., De Brito, J., & Hawreen, A. (2020). Fresh properties of recycled aggregate concrete. Construction and Building Materials, 233, 117322. https://doi.org/https://doi.org/10.1016/j.conbuildmat.2019.117322

Lee, G. C., & Choi, H. B. (2013). Study on interfacial transition zone properties of recycled aggregate by micro-hardness test. Construction and Building Materials, 40, 455-460. https://doi.org/https://doi.org/10.1016/j.conbuildmat.2012.09.114

Mills-Beale, J., & You, Z. (2010). The mechanical properties of asphalt mixtures with recycled concrete aggregates. Construction and Building Materials, 24(3), 230–235.

Mirza, F. A., & Saif, M. A. (2010, 2010). Mechanical properties of recycled aggregate concrete incorporating silica fume. Proceedings of the 2nd International Conference on Sustainable Construction Materials and Technologies,

Mueller, A., & Winkler, A. (1998, 1998). Characteristics of processed concrete rubble. Sustainable Construction: Use of Recycled Concrete Aggregate: Proceedings of the International Symposium organised by the Concrete Technology Unit, University of Dundee and held at the Department of Trade and Industry Conference Centre, London, UK on 11–12 November 1998,

Nazarimofrad, E., Shaikh, F. U. A., & Nili, M. (2017). Effects of steel fibre and silica fume on impact behaviour of recycled aggregate concrete. Journal of Sustainable Cement-Based Materials, 6(1), 54-68. https://doi.org/10.1080/21650373.2016.1230900

Pang, B., Zheng, H., Jin, Z., Hou, D., Zhang, Y., Song, X., Sun, Y., Liu, Z., She, W., Yang, L., & Li, M. (2024). Inner superhydrophobic materials based on waste fly ash: Microstructural morphology of microetching effects. Composites Part B: Engineering, 268, 111089. https://doi.org/https://doi.org/10.1016/j.compositesb.2023.111089

Pradhan, S., Kumar, S., & Barai, S. V. (2020). Multi-scale characterisation of recycled aggregate concrete and prediction of its performance. Cement and Concrete Composites, 106, 103480.

Qudoos, A., Kim, H. G., & Ryou, J.-S. (2018). Influence of the surface roughness of crushed natural aggregates on the microhardness of the interfacial transition zone of concrete with mineral admixtures and polymer latex. Construction and Building Materials, 168, 946–957.

Rahman Sobuz, M. H., Alam, A., John Oehlers, D., Visintin, P., Hamid Sheikh, A., Mohamed Ali, M. S., & Griffith, M. (2023). Experimental and analytical studies of size effects on compressive ductility response of Ultra-High-Performance Fiber-Reinforced concrete. Construction and Building Materials, 409, 133864. https://doi.org/https://doi.org/10.1016/j.conbuildmat.2023.133864

Rahman Sobuz, M. H., Meraz, M. M., Safayet, M. A., Mim, N. J., Mehedi, M. T., Noroozinejad Farsangi, E., Shrestha, R. K., Kader Arafin, S. A., Bibi, T., Hussain, M. S., Bhattacharya, B., Aftab, M. R., Paul, S. K., Paul, P., & Meraz, M. M. (2023). Performance evaluation of high-performance self-compacting concrete with waste glass aggregate and metakaolin. Journal of Building Engineering, 67, 105976. https://doi.org/https://doi.org/10.1016/j.jobe.2023.105976

Rana, M. J., Hasan, M. R., & Sobuz, M. H. R. (2022). An investigation on the impact of shading devices on energy consumption of commercial buildings in the contexts of subtropical climate. Smart and Sustainable Built Environment, 11(3), 661-691. https://doi.org/10.1108/SASBE-09-2020-0131

Rao, M. C., Bhattacharyya, S. K., & Barai, S. V. (2011). Behaviour of recycled aggregate concrete under drop weight impact load. Construction and Building Materials, 25(1), 69–80.

Saravanakumar, P., Abhiram, K., & Manoj, B. (2016). Properties of treated recycled aggregates and its influence on concrete strength characteristics. Construction and Building Materials, 111, 611-617. https://doi.org/https://doi.org/10.1016/j.conbuildmat.2016.02.064

Sasanipour, H., & Aslani, F. (2020). Durability properties evaluation of self-compacting concrete prepared with waste fine and coarse recycled concrete aggregates. Construction and Building Materials, 236, 117540.

Silva, Y. F., Delvasto, S., Izquierdo, S., & Araya-Letelier, G. (2021). Short and long-term physical and mechanical characterization of self-compacting concrete made with masonry and concrete residue. Construction and Building Materials, 312, 125382.

Sinduja Joseph, H., Pachiappan, T., Departamento de Ingeniería Civil, Universidad de Concepción, Concepción (Chile), Avudaiappan, S., Departamento de Ingeniería Civil, Universidad de Concepción, Concepción (Chile), Guindos, P., & Department of Structural & Geotechnical Engineering, Pontificia

Universidad Católica de Chile. (2023). Prediction of the mechanical properties of concrete incorporating simultaneous utilization of fine and coarse recycled aggregate. Revista de La Construcción, 22(1), 178–191. https://doi.org/10.7764/RDLC.22.1.178

Singh, H., & Ishfaq, M. (2019). Durability Property of Self Compacting Concrete with Recycled Aggregate and Silica Fume. In H. Singh, P. Garg, I. Kaur, H. Singh, P. Garg, & I. Kaur (Eds.), Proceedings of the 1st International Conference on Sustainable Waste Management through Design (Vol. 21, pp. 250-263). http://link.springer.com/10.1007/978-3-030-02707-0_31

Sobuz, M. H. R., Al, I., Datta, S. D., Jabin, J. A., Aditto, F. S., Sadiqul Hasan, N. M., Hasan, M., & Zaman, A. A. U. (2024). Assessing the influence of sugarcane bagasse ash for the production of eco-friendly concrete: Experimental and machine learning approaches. Case Studies in Construction Materials, 20, e02839. https://doi.org/https://doi.org/10.1016/j.cscm.2023.e02839

Sobuz, M. H. R., Datta, S. D., & Akid, A. S. M. (2023). Investigating the combined effect of aggregate size and sulphate attack on producing sustainable recycled aggregate concrete. Australian Journal of Civil Engineering, 21(2), 224-239. https://doi.org/10.1080/14488353.2022.2088646

Sobuz, M. H. R., Datta, S. D., Akid, A. S. M., Tam, V. W. Y., Islam, S., Rana, M. J., Aslani, F., Yalçınkaya, Ç., & Sutan, N. M. (2022). Evaluating the effects of recycled concrete aggregate size and concentration on properties of high-strength sustainable concrete. Journal of King Saud University-Engineering Sciences. https://doi.org/https://doi.org/10.1016/j.jksues.2022.04.004

Sobuz, M. H. R., Datta, S. D., & Rahman, M. (2022). Evaluating the Properties of Demolished Aggregate Concrete with Non-destructive Assessment. In S. Arthur, M. Saitoh, & S. K. Pal (Eds.), Advances in Civil Engineering, Lecture Notes in Civil Engineering (pp. 223-233). Springer Singapore. https://doi.org/10.1007/978-981-16-5547-0_22

Sobuz, M. H. R., Joy, L. P., Akid, A. S. M., Aditto, F. S., Jabin, J. A., Hasan, N. M. S., Meraz, M. M., Kabbo, M. K. I., & Datta, S. D. (2024). Optimization of recycled rubber self-compacting concrete: Experimental findings and machine learning-based evaluation. Heliyon, 10(6), e27793. https://doi.org/https://doi.org/10.1016/j.heliyon.2024.e27793

Song, X., Wang, W., Deng, Y., Su, Y., Jia, F., Zaheer, Q., & Long, X. (2024). Data-driven modeling for residual velocity of projectile penetrating reinforced concrete slabs. Engineering Structures, 306, 117761. https://doi.org/https://doi.org/10.1016/j.engstruct.2024.117761

Standard, A. (2001). Concrete structures. AS-3600. Sydney: Standards Australia International. http://www.singaporestandardseshop.sg/data/ECopyFileStore/081014164134Preview%20-%20SS%20EN%201992-1-1-2008.pdf

Tang, Y., Feng, W., Chen, Z., Nong, Y., Guan, S., & Sun, J. (2021). Fracture behavior of a sustainable material: Recycled concrete with waste crumb rubber subjected to elevated temperatures. Journal of Cleaner Production, 318, 128553.

Wei, C., Li, Y., Liu, X., Zhang, Z., Wu, P., & Gu, J. (2024). Large-scale application of coal gasification slag in nonburnt bricks: Hydration characteristics and mechanism analysis. Construction and Building Materials, 421, 135674. https://doi.org/https://doi.org/10.1016/j.conbuildmat.2024.135674

Wei, J., Ying, H., Yang, Y., Zhang, W., Yuan, H., & Zhou, J. (2023). Seismic performance of concrete-filled steel tubular composite columns with ultra-high performance concrete plates. Engineering Structures, 278, 115500. https://doi.org/https://doi.org/10.1016/j.engstruct.2022.115500

Wu, P., Liu, X., Zhang, Z., Wei, C., Wang, J., & Gu, J. (2024). The harmless and value-added utilization of red mud: Recovering iron from red mud by pyrometallurgy and preparing cementitious materials with its tailings. Journal of Industrial and Engineering Chemistry, 132, 50-65. https://doi.org/https://doi.org/10.1016/j.jiec.2023.11.038

Xie, J., Fang, C., Lu, Z., Li, Z., & Li, L. (2018). Effects of the addition of silica fume and rubber particles on the compressive behaviour of recycled aggregate concrete with steel fibres. Journal of Cleaner Production, 197, 656–667.

Xie, J., Huang, L., Guo, Y., Li, Z., Fang, C., Li, L., & Wang, J. (2018). Experimental study on the compressive and flexural behaviour of recycled aggregate concrete modified with silica fume and fibres. Construction and Building Materials, 178, 612–623.

Younis, K. H., Alzeebaree, R., Ismail, A. J., Khoshnaw, G. J., & Ibrahim, T. K. (2021, 2021). Performance of Recycled Coarse Aggregate Concrete Incorporating Metakaolin. IOP Conference Series: Earth and Environmental Science,

Younis, K. H., & Pilakoutas, K. (2013). Strength prediction model and methods for improving recycled aggregate concrete. Construction and Building Materials, 49, 688–701.

Younis, K. H., Pilakoutas, K., Guadagnini, M., & Angelakopoulos, H. (2014, 2014). Feasibility of using recycled steel fibres to enhance the behavior of recycled aggregate concrete. FRC 2014 Joint ACI-Fib International Workshop-Fibre Reinforced Concrete: From Design to Structural Applications,

Yunchao, T., Zheng, C., Wanhui, F., Yumei, N., Cong, L., & Jieming, C. (2021). Combined effects of nano-silica and silica fume on the mechanical behavior of recycled aggregate concrete. Nanotechnology Reviews, 10(1), 819-838. https://doi.org/10.1515/ntrev-2021-0058

Zhang, W., Lin, J., Huang, Y., Lin, B., & Kang, S. (2024). Temperature-dependent debonding behavior of adhesively bonded CFRP-UHPC interface. Composite Structures, 340, 118200. https://doi.org/https://doi.org/10.1016/j.compstruct.2024.118200

Zhao, R., Li, C., & Guan, X. (2024). Advances in Modeling Surface Chloride Concentrations in Concrete Serving in the Marine Environment: A Mini Review. Buildings, 14(6), 1879. https://www.mdpi.com/2075-5309/14/6/1879